



REDUCED RESISTANCE OF MICROWAVE IRRADIATED Sn DOPED CdO NANOSTRUCTURES FOR CHEMORESISTIVE GAS SENSORS

N.RAJESH

PG Assistant, Department of Physics,
Government Higher Secondary School,
Palayajayankondam, Karur, Tamilnadu – 639102, INDIA

Abstract - Highly conducting tin doped cadmium oxide nanostructures were synthesized by cost effective and energy efficient microwave assisted wet chemical technique for chemoresistive gas sensors. The doping percentage of Sn with CdO is varied from 1 to 10 wt%. The average crystalline size of undoped and tin doped cadmium oxide nanostructures were calculated from X-ray diffraction (XRD) pattern and found to be in the ranges from 51–12 nm. Also it was confirmed from transmission electron microscopy (TEM) analysis. The presence of chemical composition of undoped and Sn doped CdO nanostructures were recorded by EDS spectrum. The Sn doped CdO nanostructures demonstrated obviously improved crystalline quality, reduced average crystallite size and reduced resistance. Among the various doping concentrations of Sn with CdO from 1 to 10 wt%, the 1 wt% of Sn doped CdO nanostructures shows the lower resistance of 2.67 Ω . This resistance is about 90 % lower than the resistance of undoped CdO nanostructures. The improvement of electrical properties endow that the Sn doped CdO nanostructures have potential applications in chemoresistive gas sensors.

Keywords: Nanostructured materials; Oxide materials; Chemical synthesis; Transmission electron microscopy; Gas sensing properties.

I. INTRODUCTION

Fifty years ago chemoresistive gas sensors were introduced for the first time. Today, the development of semiconducting sensing materials is adjunctively reliant on opportunities provided by new nanoscale technologies. Nanoscience, enabling controllable

manipulation of matter at the molecular level, has become a fundamental generator for innovations in materials processing. Furthermore, emerging nanotechnologies promise dramatic changes in sensor designs and capabilities [1]. At present, there has been considerable interest to develop the semiconducting metal oxides. Nanostructured materials have attracted the attention of researchers not only by their unique chemical and physical properties but also by their potential application in many fields, which has stimulated the search for new synthetic methods for these materials. Among the metal oxides CdO is one of the effective material for potential applications. Undoped CdO is an n-type semiconductor with the band gap in the range of 2.2–2.8 eV and possesses low resistivity (10^{-2} - 10^{-4} Ω cm) due to the defect of oxygen vacancies and cadmium interstitials [2-5]. Doping the metal oxide layer with suitable promoters (metal particles, foreign metal oxide, ions) is a common way of enhancing the sensing characteristics of chemoresistive gas sensors. The conductivity of the undoped CdO can be increased by adding suitable dopant having ionic radii smaller or equal to that of host lattice atoms [6]. The Sn is a promising material, which is substitute in the CdO crystal should improve the electrical properties [7]. Undoped and tin doped CdO with various dopants has been reported using different methods viz. pulse laser deposition [7], chemical vapor deposition [8], chemical bath deposition [9], ultrasonic spray [10], sol-gel [11], vacuum evaporation [12], spray pyrolysis technique [13], thermal evaporation [14], and electrochemical method [15].

The above mentioned methods were required high budget, post-synthesis of heating, high energy and huge time consumption to prepare undoped and Sn doped CdO nanostructures. In the present work, microwave



assisted method [16-18] is used to prepare Sn doped CdO nanostructures for chemoresistive gas sensors. In this method, good quality product of undoped and Sn doped CdO nanostructures have been obtained in just 15 min without post synthesis of heating process. The microwave assisted wet chemical route has many advantages such as: (a) reduction of process temperature and time; (b) an increased productivity; (c) a reduction of energy consumption and (d) relatively inexpensive. Investigation of Sn doped CdO nanostructure using microwave assisted wet chemical route, seems to be quite fascinating and encouraging one.

II. EXPERIMENTAL

A. Synthesis

The cadmium acetate and stannous chloride were taken as precursor material. Each 0.1 M concentration of precursor solutions was prepared separately. The obtained solutions were mixed (Stannous chloride precursor solution was added drop wise into cadmium acetate precursor solution) together in different stoichiometric ratios (Sn 1, 3, 5, 7 and 10 wt%). Then the solution is neutralized with ammonia solution and pH of the solution is maintained at 8. The resulting solutions were washed with double distilled water more than 5 times to reduce impurities. The resulting precipitate was placed in a microwave oven (2.45 GHz, 800 W) and irradiated for 15 min. Finally the solution was dried at 120 °C in air.

B. Characterization

The crystalline structure of the samples was analyzed by X-ray diffraction (XRD) through Bruker AXS D8 advance instrument and using $\text{CuK}\alpha_1$ wavelength of 1.5406 Å. High resolution transmission electron microscopy (HRTEM) and EDS spectrum was recorded on a TechnaiG20-stwin using an accelerating voltage of 200 kV. N4lthase sensitive impedance analyzer was used to measure electrical resistance of the samples.

III. RESULTS AND DISCUSSION

A. X-ray diffraction

The structural properties of CdO nanostructures before and after incorporation of Sn were investigated by XRD analysis. Fig. 1 depicts the XRD patterns of undoped and Sn doped CdO nanostructures were synthesized by microwave-assisted technique. The XRD data for all the samples were acquired at room temperature (298 K).

The diffraction pattern of the as-prepared undoped CdO sample revealed the formation of face centered cubic structure, the Miller indices are (111), (200), (220), (311), (222) and the diffraction patterns are well matches with JCPDS card #65-2908 [17]. No extra peaks were observed which indicates the absence of other impure phases.

The average crystalline size of the samples were determined using Scherrer formula,

$$d = \frac{k\lambda}{\beta \cos \theta} \quad \text{----- (1)}$$

where d is average crystalline size, K is shape factor (K = 0.9), λ is wavelength of X-ray used for analysis ($\lambda = 1.54 \text{ \AA}$), β is the full width half maximum and θ is the diffraction angle. Initially, the crystalline size decreases with adding the concentration of Sn. The crystalline size 51 nm and 12 nm were observed for undoped and 1 % of Sn doped CdO nanostructures, respectively. This evolution can be due to the disorder creates in the crystal lattice by the incorporation of the Sn ions. Also broadening of peaks in the XRD spectra was observed for 1 wt% of Sn doped CdO sample relative to undoped CdO. However, further increases of Sn concentration the FWHM decreases suggesting an increase of the crystalline size (16 – 30 nm). Further, sharpness of diffraction peaks observed for higher concentration of Sn (3 – 10 % of Sn). The lattice parameter, diffraction angle, average crystalline size and d spacing of undoped and Sn doped CdO nanostructures are given in Table. 1. The lattice parameter were calculated using Eq. (2)

$$d = \frac{a}{\sqrt{(h^2 + k^2 + l^2)}} \quad \text{----- (2)}$$

The peaks of 1 wt% of Sn doped CdO sample is slightly shifted relative to undoped CdO towards lower Bragg angles and the lattice parameter is also changed. It can be observed that increasing of lattice parameter and expansion of unit cell, as given in Table 1. This is due to atomic radii of Sn^{2+} (1.18 Å) and Cd^{2+} (0.97 Å) ions. Further the doping concentration increases above 1 wt% of Sn, that there is a slight shift of diffraction peaks towards higher Bragg angle. It can be observed that the reduction of lattice parameter which is due to substitution of Sn in Cd position in the CdO crystal

Table. 1 The lattice parameters, 2theta, average crystalline and d-spacing of undoped and Sn doped

CdO nanostructure at different Sn doping concentrations.

Sample	Lattice parameter a (Å)	2θ ₍₁₁₁₎ (deg)	Average crystalline (nm)	d-spacing (111) value
Undoped CdO	4.6961	33.01	51	2.7113
Sn 1%	4.7771	32.44	12	2.7581
Sn 3%	4.7741	32.45	16	2.7563
Sn 5%	4.7708	32.47	21	2.7544
Sn 7%	4.7700	32.48	25	2.7524
Sn 10%	4.7681	32.49	30	2.7502

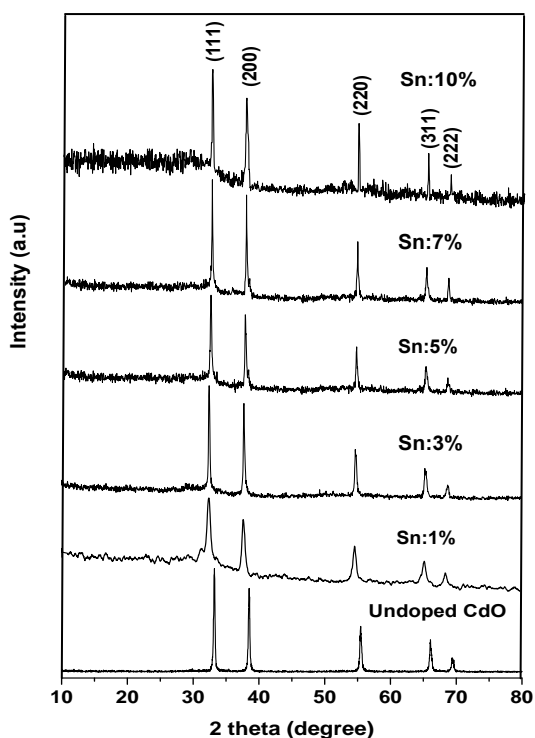


Fig. 1. XRD pattern of undoped and Sn doped CdO nanostructure at different Sn doping concentrations.

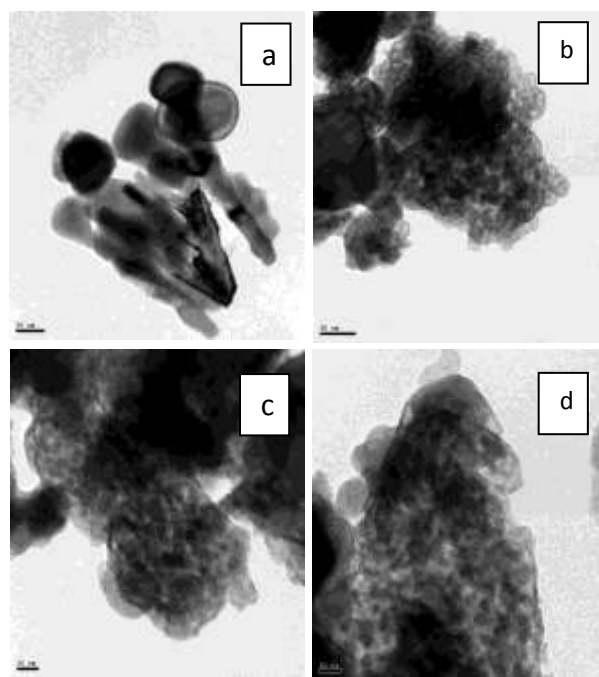
B. Transmission electron microscope

Fig. 2a–d shows TEM micrographs related to undoped and 1 % Sn-doped CdO nanostructures. TEM micrograph in Fig. 2a shows the rod like surface morphology of undoped CdO nanostructures, having

thickness 26 nm and length has few μm. Fig. 2b-d shows the agglomerated spherical shaped particles of 1 wt% of Sn doped CdO nanostructures with sizes of 10 nm.

Fig.2 (a) TEM image of undoped CdO, (b,c,d) Sn doped CdO nanostructures

This evolution of surface morphology can be due to the incorporation of the Sn ions in CdO lattice. The 15 min of microwave irradiation accelerates the surface morphology of CdO into unidirectional growth. But the concentration of Sn added with CdO, it control



unidirectional growth and produce spherical shaped morphology. Particle size observed from TEM analysis supported to XRD results.

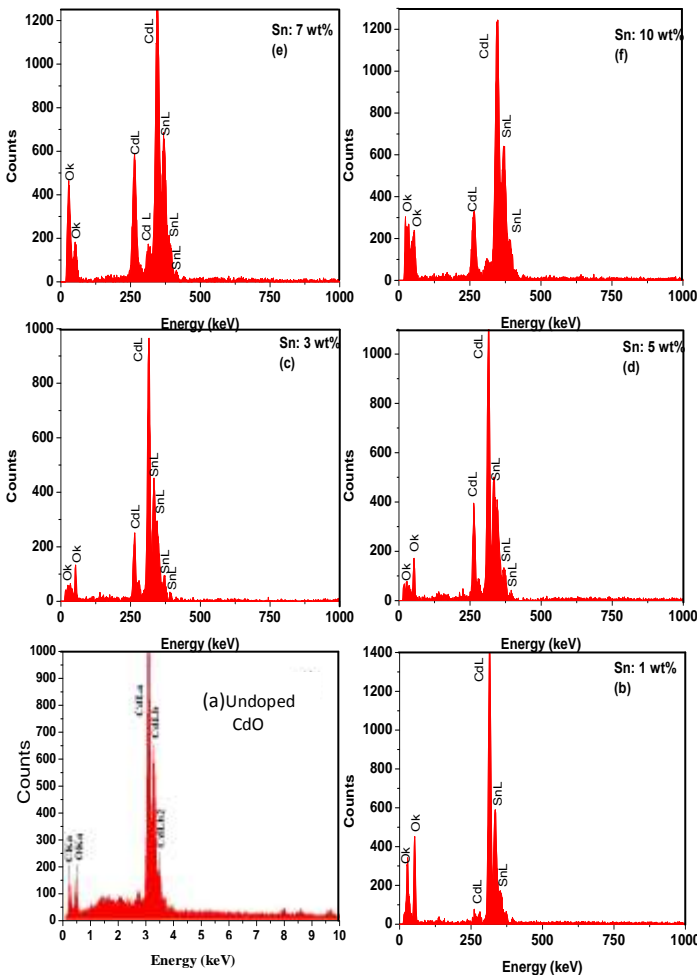
C. Energy dispersive analysis

EDS analysis (Fig. 3a–f) was carried out to investigate the elemental composition of undoped and Sn doped CdO nanostructures. Fig. 3a reports the spectrum of undoped CdO, showing the characteristic peaks associated with O and Cd elements and the low intensity carbon peak is likely to be produced during chemical decomposition of the cadmium precursor [19]. The measured atomic percentage of these elements are



9.74 at.% (O) ,82.53 at.% (Cd) and 7.73 at.% (C). Fig. 3b-f shows EDS analysis of Sn doped CdO nanostructures. The measured Sn contents are about 1.7, 12.71, 16.94, 23.11 and 31.71 at.% respectively, for the five nominal compositions of 1, 3, 5, 7 and 10 wt%, indicating that the experimental Sn percentage in the samples is consistently higher than the nominal loading one. This study confirms Sn ions are successfully substituted in the CdO lattice. No evidence of other impurities was found and these data also confirm the purity of the Sn doped CdO nanostructures.

Fig. 3. EDS spectrum of undoped and Sn doped CdO nanostructure at different Sn doping concentrations



D. Electrical resistance

Fig. 4 shows the variations of the electrical resistance of undoped and Sn doped CdO nanostructures with different concentrations of Sn. The undoped CdO sample has the resistance of 174.72 MΩ and 1 wt % of Sn doped CdO samples shows the minimum resistance value of 2.67 Ω. This resistance is much lower than the undoped CdO samples. Then, the resistance began to increase as the amounts of Sn concentration increases further to 3, 5, 7 and 10 wt%. Such lower resistance of 1 % of Sn doped CdO sample may occurs due to the substitution of cadmium ions by Sn ions may occupy the interstitial site in the lattice. For each substitution of Sn ions in CdO can liberate two free electrons in the conduction band, which can enhance the free charge carrier concentration significantly.

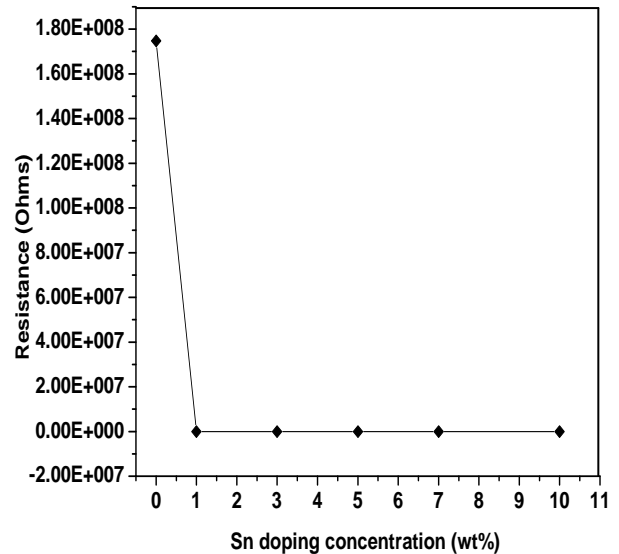


Fig. 4. Variation of resistance with different concentrations of Sn doping in cadmium oxide nanostructure

As a result, the resistance decreases abruptly i.e., the resistance value is about 10⁷ times decreases comparing to undoped CdO. However, when Sn concentration increases to 3 % and higher, the resistance of the samples starts to increases as shown in Fig. 4.

E. I-V Characteristics



Fig. 5 shows the current voltage (I–V) characteristics of 1 % of Sn doped CdO nanostructures synthesized by microwave irradiation technique at 15 min of irradiation time. From the figure, the current increases linearly with applied voltage. It was observed to be nearly symmetrical in nature indicating ohmic nature of contacts. The non-linear I–V characteristics may be due to semiconducting nature of material. The variation of resistance in air is attributed to the effect of oxygen chemisorption. This is generally accepted that oxygen is chemisorbed at a surface site such as oxygen vacancy in the form of an ionized oxygen atom or molecule, i.e. O^- or O_2^- , resulting in a reduced concentration of free electrons at the surface and the observed reduction in the conductivity [20].

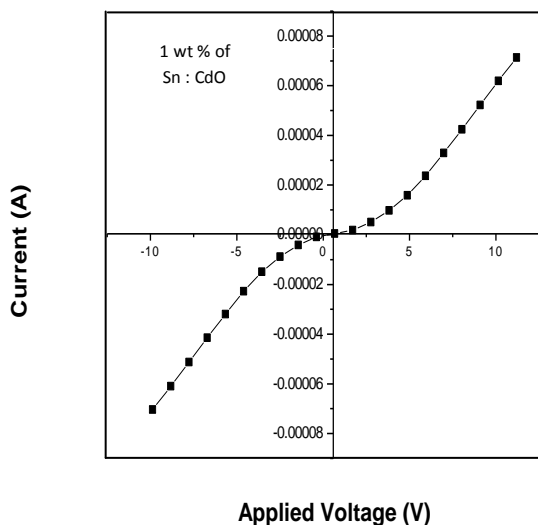


Fig. 5. I–V characteristics of 1 wt % of Sn doped CdO nanostructures

Metal oxide sensors are also known as chemiresistors. The detection principle of resistive sensors is based on change of the resistance of a material upon adsorption of the gas molecules on the surface of a semiconductor. The gas-solid interactions affect the resistance of the material because of the density of electronic species in the material. Metal oxide semiconductors demonstrate good detection sensitivity, robustness and the ability to withstand high temperatures and the technique is commonly used to monitor a variety of toxic and inflammable gases in a variety of air pollution

monitoring systems, the food industry, medical diagnosis equipment and gas leak alarms.

A chemoresistive sensor is based on a sensitive material, in bulk or deposited on a suitable support, upon which the molecular recognition process takes place. The analyte recognition process occurs either at the surface of the sensing element or in the bulk of the material, leading to a concentration-dependent change property that can be transformed into an electrical signal by the appropriate transducer. This simple transduction mechanism allowed the fabrication of devices with different configurations. Table.2 illustrates the main characteristics of chemoresistive, electrochemical and optical gas sensors. Detection of target gases by chemoresistive gas sensors has received impulse great deal of attention because of its many advantages over other sensing technologies [21].

Electrochemical sensors are becoming unpopular as they have a short lifetime, rendering them unacceptable for some applications. Optical sensors show excellent characteristics of sensitivity, adequate lifetime, and fast response; however, they have a high cost and large size. Although the chemoresistive sensors are low cost and fabrication simplicity of chemoresistive sensors are the main factors contributing to their widespread use [21].

The target gas interacts with the surface of the metal oxide, which results in a change in charge carrier concentration of the material. This change in charge carrier concentration serves to alter the conductivity or resistivity of the material. An n-type semiconductor is one where the majority charge carriers are electrons, and upon interaction with a reducing gas an increase in conductivity occurs. Conversely, an oxidising gas serves to deplete the sensing layer of charge carrying electrons, resulting in a decrease in conductivity. A p-type semiconductor is a material that conducts with positive holes being the majority charge carriers; hence, the opposite effects are observed with the material and showing an increase in conductivity in the presence of an oxidising gas (where the gas has increased the number of positive holes). A resistance increase with a reducing gas is observed, where the negative charge introduced in to the material reduces the positive (hole) charge carrier concentration [22]. A summary of the response of the material is provided in Table.3



Table.2 Comparison of three types of gas sensors

Characteristic	Chemo-resistive	Electro-chemical	Optical
Cost	low	low	high
Lifetime	long	short	long
Sensitivity	high	high	high
Response time	fast	fast	fast
Size	small	medium	large

Table.3 Sign of resistance change to change in gas atmosphere

Classification	Oxidising Gases	Reducing Gases
n-type	Resistance increases	Resistance decreases
p-type	Resistance decreases	Resistance increases

The grain-size reduction at nanometric level and doping the metal oxide layer with suitable promoters are a common way of enhancing the sensing characteristics of chemoresistive gas sensors. It is in fact well recognized that by reducing the particle size of the sensing material in the nanometer range the sensitivity of chemoresistive gas sensors is greatly improved both for the large specific surface offered and for the influence in reducing the surface charge density [23-31]. Furthermore, in this size range, a large fraction of the atoms (up to 50%) are present at the surface or the interface region; therefore, the chemical and electronic of nanoparticles are different from those of the bulk, consequently contributing to an increase in the sensing properties.

In this present work, the size of synthesized material were reduced to 10 nm (1 wt% of Sn doped CdO) and Sn ions were successfully incorporate with CdO nanostructures, hence 1 wt% of Sn doped CdO nanostructures exhibits the lowest resistance value. As a result the material offers large numbers of electrons present in surface states. The synthesized material exposed to target gases, it exhibit greater conductance changes as more carriers are activated from their trapped states to the conduction band. It is possible to enhance sensor response even at low ppm level of concentration by using our material. It has been

strongly suggested 1wt % of Sn doped CdO nanostructure is used to detect variety of oxidizing and reducing gases

IV. CONCLUSION

Undoped and low resistive tin doped CdO nanoparticles were obtained by microwave assisted wet chemical technique from starting solution of SnCl₂ and Cd(COOCH₃)₂.2H₂O. XRD measurements revealed that all the concentration of Sn successfully incorporate with CdO, also all the products were exhibited face centered cubic crystalline structure with slight variation of lattice parameter due to the substitution of Cd by Sn ions. The formation of single crystalline undoped and tin doped CdO nanoparticles has been confirmed by TEM micrograph. TEM analysis strongly supported to XRD results. EDS spectrum exhibited chemical composition of Sn doped CdO with different concentrations. The lower concentration 1 wt% of Sn doped CdO nanostructures shows lower electrical resistance of 2.67 Ω, due to the replacement of Cd by Sn ions in CdO lattice, which can liberate free electrons in the conduction band and hence enhance conductivity significantly. Finally, 1 wt% of Sn doped CdO nanostructures is strongly recommended for detecting oxidizing and reducing gases at sub level ppm concentration due to significant electrical property of this material.

V. REFERENCE

- [1] N. Barsan, M. Schweizer-Berberich, W. Gopel, "Fundamental and practical aspects in the design of nanoscaled SnO₂ gas sensors: a status report," *Fresenius J. Anal. Chem.*, vol. 365, pp. 287-304, 1999.
- [2] P.H. Jefferson, S.A. Hatfield, T.D. Veal, P.D.C. King, C.F. McConville, J. Zuniga- Perez, V. Munoz-Sanjose, "Band-gap and Effective Mass Determination of Epitaxial CdO," *Appl. Phys. Lett.* Vol. 92, pp. 022101, 2008.
- [3] Y.S. Choi, C.G. Lee, S.M. Cho, "Transparent conducting Zn_xCd_{1-x}O thin films prepared by the sol-gel process," *Thin Solid Films*, vol. 289, pp. 153-158, 1996.
- [4] J.S. Cruz, G.T. Delgado, R.C. Perez, S.J. Sandoval, O.J. Sandoval, C.I.Z. Romero, J.M. Marin, O.Z. Angel, "Dependence of electrical and optical properties of sol-gel prepared undoped cadmium oxide thin films on annealing temperature," *Thin Solid Films*, vol. 493, pp. 83-87, 2005.



- [5] Y. Yang, S.J. Shu, J.E. Medvedeva, J.R. Ireland, A.W. Metz, Ni. Jun, M.C. Hersam, A.J. Freeman, T.J. Marks, "CdO as the archetypical transparent conducting oxide. systematics of dopant ionic radius and electronic structure effects on charge transport and band structure," *Am. Chem. Soc.*, vol. 127, pp. 8796-8804, 2005.
- [6] B.J. Zheng, J.S. Lian, L. Zhao, Q. Jiang, "Optical and electrical properties of Sn-doped CdO thin films obtained by pulse laser deposition," *Vacuum*. Vol. 85, pp. 861-865, 2011.
- [7] Z. Zhao, D.L. Morel, C.S. Ferekides, "Electrical and optical properties of tin-doped CdO films deposited by atmospheric metalorganic chemical vapor deposition," *Thin Solid Films*, vol. 413, pp. 203-211, 2002.
- [8] L.R. de Leon Gutierrez, J.J. Cayente Romeo, J.M. Peza Tapia, E. Barrera Calva, J.C. Martienz Flores, M. Ortega Lopez, "Some physical properties of Sn-doped CdO thin films prepared by chemical bath deposition," *Mater. Lett.*, vol. 60, pp. 3866-3870, 2006.
- [9] S. Kose, F. Atay, V. Bilgin, I. Akyuz, "In doped CdO films: Electrical, optical, structural and surface properties," *Int. J. Hydrogen Energy*, vol.34, pp. 5260-5266, 2009.
- [10] R. Maity, K.K. Chattopadhyay, "Synthesis and characterization of aluminum-doped CdO thin films by sol-gel process," *Sol. Energy Mater. Sol. Cells*, vol. 90, pp. 597-606, 2006.
- [11] R.S. De Biasi, M.L.N. Grillo, "Influence of manganese concentration on the electron magnetic resonance spectrum of Mn^{2+} in CdO," *J. Alloys Compd.*, vol.485, pp. 26-28, 2009.
- [12] P.M. Devshette, N.G. Deshpande, G.K. Bichile, "Growth and physical properties of $Zn_xCd_{1-x}O$ thin films prepared by spray pyrolysis technique," *J. Alloys Compd.*, vol. 463, pp. 576-580, 2008.
- [13] C. Dantus, G.G. Rusu, M. Dobromir, M. Rusu, "Preparation and characterization of CdO thin films obtained by thermal oxidation of evaporated Cd thin films," *Appl. Surf. Sci.*, vol. 255, pp. 2665-2670, 2008.
- [14] R. Henriquez, P. Grez, E. Munoz, J.A. Badan, R.E. Marotti, E.A. Dalchiele, "Optical properties of CdSe and CdO thin films electrochemically prepared," *Thin Solid Films*, vol. 518, pp. 1774-1778, 2010.
- [15] O. Vigil, F. Cruz, A. Morales-Acevedo, G. Contreras-Puente, L. Vaillant, G. Santana, "Structural and optical properties of annealed CdO thin films prepared by spray pyrolysis," *Mater. Chem. Phys.*, vol. 68, pp. 249 – 252, 2001.
- [16] N. Rajesh, J.C. Kannan, T. Krishnakumar, S.G. Leonardi, G. Neri, "Sensing behavior to ethanol of tin oxide nanoparticles prepared by microwave synthesis with different irradiation time," *Sens. Actuators B*, vol.194, pp. 96 – 104, 2014.
- [17] N. Rajesh, J.C. Kannan, S.G. Leonardi, G. Neri, T. Krishnakumar, "Investigation of CdO nanostructures synthesized by microwave assisted irradiation technique for NO_2 gas detection," *J. alloy. Compd.*, vol. 607, pp. 54 – 60, 2014.
- [18] N. Rajesh, J.C. Kannan, T. Krishnakumar, G. Neri, "Microwave irradiation effect on structural, optical, and thermal properties of cadmium oxide nanostructure," *Acta Phys. Pol. A*, vo. 125, pp. 1229 – 1235, 2014.
- [19] Barbara Malecka, Agnieszka Lacz, "Thermal decomposition of cadmium formate in inert and oxidative atmosphere," *Thermochim. Acta*, vol. 479, pp. 12–16, 2008.
- [20] N. H. Al-Hardan, M. J. Abdullah, A. Abdul Aziz, "Sensing mechanism of hydrogen gas sensor based on RF- sputtered ZnO thin films," *Int. J. Hydrogen Energ.*, vol. 35, pp. 4428 – 4434, 2010.
- [21] Giovanni Neri, "First Fifty Years of Chemosensitive Gas Sensors," *Chemosensors*, vol. 3, pp. 1-20, 2015.
- [22] George F. Fine, Leon M. Cavanagh, Ayo Afonja, Russell Binions, "Metal Oxide Semi-Conductor Gas Sensors in Environmental Monitoring," *Sensors*, vol.10, pp. 5469-5502, 2010.
- [23] G. Korotcenkov, "Gas response control through structural and chemical modification of metal oxide films: State of the art and approaches," *Sens. Actuators B Chem*, vol.107, pp. 209–232, 2005.
- [24] M.I. Baraton, L. Merhari, "Influence of the particle size on the surface reactivity and gas sensing properties of SnO_2 nanopowders," *Mater. Trans.*, vol. 42, pp. 1616–1622, 2001.
- [25] C. Xu, J. Tamaki, N. Miura, N. Yamazoe, "Grain size effects on gas sensitivity of porous SnO_2 -based elements," *Sens. Actuators B Chem*, vol. 3, pp. 147–155, 1991.
- [26] R. Dolbec, M.A. Khakani, A.M. Serventi, R.G. Saint-Jacques, "Influence of the nanostructural characteristics on the gas sensing properties of pulsed laser deposited tin oxide thin films," *Sens. Actuators B Chem*, vol. 93, pp. 566–571, 2003.
- [27] A. Gurlo, M. Ivanovskaya, N. Barsan, M. Schweizer-Berberich, U. Weimar, W. Gopel, A. Dieguez, "Grain size control in nanocrystalline In_2O_3 semiconductor gas sensors," *Sens. Actuators B Chem*, vol. 44, pp. 327–333, 1997.



- [28] S.G. Ansari, P. Boroojerdian, S.R. Sainkar, R.N. Karekar, R.C. Aiyer, S.K. Kulkarni, "Grain size effects on H₂ gas sensitivity of thick film resistor using SnO₂ nanoparticles," *Thin Solid Films*, vol. 295, pp. 271–276, 1997.
- [29] A. Dieguez, A. Romano-Rodriguez, J.R. Morante, U. Weimar, M. Schweizer-Berberich, W. Gopel, "Morphological analysis of nanocrystalline SnO₂ for gas sensor applications," *Sens. Actuators B*, vol.31, pp.1–8, 1996.
- [30] G. Korotcenkov, "The role of morphology and crystallographic structure of metal oxides in response of conductometric-type gas sensors," *Mater. Sci. Eng. R*, vol. 61, pp. 1–39, 2008.
- [31] A. Rothschild, Y. Komem, "Metal oxide gas sensors with nanosized grains," *J. Electroceram*, vol.13,pp.697–701,2004.